Chemical Engineering Journal 428 (2022) 132625

Contents lists available at ScienceDirect

Chemical Engineering Journal

journal homepage: www.elsevier.com/locate/cej

In-situ electro-polymerization of fluorescent electrochromic thin films based on charge-transfer complexes

Jingwei Sun [a], Shengchen Yang [a,*], Jiali Wu [a], Xixi He [a], Yujian Zhang [a], Jingjing Ji [b], Cheng Zhang [c], Ziqi Liang [b,*]

[a] Department of Materials Chemistry, Huzhou University, East 2nd Ring Road No. 759, Huzhou 313000, PR China
[b] Department of Materials Science, Fudan University, 220 Handan Road, Shanghai 200433, PR China
[c] State Key Laboratory Breeding Base of Green Chemistry-Synthesis Technology, College of Chemical Engineering, Zhejiang University of Technology, Hangzhou 310014, PR China

ARTICLE INFO

Keywords:
Electro-polymerization
Charge-transfer complex
Electrochemical redox
Electrofluorochromism
Electrochromism

ABSTRACT

Fluorescent electrochromic (FEC) materials, which reversibly change their both fluorescence and absorption via electrochemical reactions in response to applied potentials, have received extensive attention. Herein we directly obtained poly (2Z,2′Z)-3,3′-(1,4-phenylene)bis(2-(4-((6-(9H-carbazol-9-yl)hexyl)oxy)phenyl)acrylonitrile) P (CHDCS) and poly (2Z,2′Z)-3,3′-(2,5-dimethoxy-1,4-phenylene)bis(2-(4-((6-(9H-carbazol-9-yl)hexyl)oxy)phenyl) acrylonitrile) P(CHDCSM) as thin films on electrodes via electro-polymerization (EP) from linear donor-acceptor (D-A) monomers with isolated π-conjugation. Surprisingly, interchain charge-transfer complexes (CTCs) with mixed D-A stacks were generated between electroactive bis-carbazole (D) and luminescent dicyanodistyrylbenzene (A) units during the EP process. Consequently, significantly redshifted and bright orange fluorescence (~600 nm) originated from intermolecular CT excitons were observed from both polymers, which could be reversibly switched upon applied potentials. This is the first time that the CTCs have been prepared via EP and applied as FEC materials. Moreover, the stronger intermolecular CT effect gives rise to an enhancement of electrical conductivity and FEC response in P(CHDCS), resulting in high optical contrasts (T = 33.6%, I_{on}/I_{off} = 28.3) and fast FEC switching (coloring 1.25 s, fading 0.53 s, quenching 2.40 s, brightening 6.17 s) as well as good reversibility. In addition, the CTCs improve the spin delocalization of bis-carbazole radical cations, leading to increased color stability of the FEC films by a decay of only 1.2% in 2 h with no power supply after coloration. This work not only affords an innovative CTC design strategy for FEC materials but also paves the way for constructing highly-performed and energy-efficient FECs via one-step electrochemical methods.

1. Introduction

Fluorescent electrochromic (FEC) materials change both fluorescence and color when a current is applied.[1,2] Polymeric FEC materials are promising candidates for applications in luminescent switches and displays, bio-probes, optical memories and smart windows owing to their unique features of light weight, flexibility, low-voltage operation and simple structural modulation.[3,4] A series of chemical syntheses of FEC polymers have been reported, such as direct polycondensation,[5] imidization,[6] oxidative polymerization,[7] Heck[8] and Suzuki[9] cross-coupling reactions. However, these chemical polymerizations require laborious synthesis, purification and film-forming procedures. Electro-polymerization (EP) is a facile one-step in-situ method that integrates synthesis with film deposition simultaneously.[10] It has been widely applied in the fabrication of electrochromic (EC) and conductive polymers.[11,12] Unfortunately, an application of the desirable EP method for FEC materials has barely achieved because the resulting polymers generally lose fluorescence due to structural defects and tight π-stacking formed during EP.[13,14]

Both Ma and Knoll groups respectively proposed effective strategies to prevent structural defects and maintain the fluorescence of EP films by constructing a cross-linked porous π-network with precursors comprising separated luminophores and electroactive moieties.[13,15,26–28] However, owing to the absent interplay between these two moieties, the fluorescence was largely irreversible or even unaffected by the redox centers.[15,16] Inspired by those past efforts, we

* Corresponding authors.
E-mail addresses: 02589@zjhu.edu.cn (S. Yang), zqliang@fudan.edu.cn (Z. Liang).

https://doi.org/10.1016/j.cej.2021.132625
Received 27 July 2021; Received in revised form 4 September 2021; Accepted 21 September 2021
Available online 25 September 2021

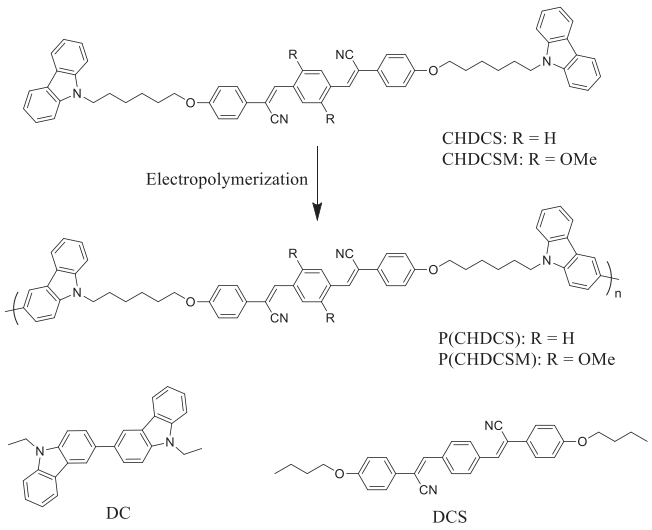

Scheme. 1. Molecular structures of the CHDCS and CHDCSM monomers, the resulting homopolymers of P(CHDCS) and P(CHDCSM), and the reference compounds DCS and DC.

propose here an exploitation of the charge-transfer complexes (CTCs) system to construct EP accessible FEC materials by adopting electroactive groups and luminophores as electron donor (D) and acceptor (A) units, respectively. CTCs are consisted of alternate stacks of D and A parts, which interact with each other through-space rather than through-bonds.[17,18] Thus, both structural defects and tight π-stacking of the luminophores could be effectively suppressed as the reactions occur in the electroactive groups. Moreover, high electrical conductivity and tunable optical properties could be obtained in CTCs, arising from the variable degree of CT at D/A interfaces.[19–22] Therefore, FEC properties are expected to achieve in CTCs that integrate both electroactive and luminescent groups, which has yet to be demonstrated. In addition, conventional CTCs with ordered hetero-molecular arrangements are generally prepared via co-crystallization, which would cause the issues of stability, reproducibility and device fabrication.[23,24] In contrast, the CTCs fabricated by the EP method have barely been reported to date.

In this work, we designed and synthesized the monomers (2Z,2′Z)-3,3′-(1,4-phenylene)bis(2-(4-((6-(9H-carbazol-9-yl)hexyl)oxy)phenyl) acrylonitrile) (CHDCS) and (2Z,2′Z)-3,3′-(2,5-dimethoxy-1,4-phenylene)bis(2-(4-((6-(9H-carbazol-9-yl)hexyl)oxy)phenyl)acrylonitrile) (CHDCSM) (Scheme 1) by end-capping fluorescent dicyanodistyrylbenzene cores with two electroactive carbazole moieties. The carbazoles and dicyanodistyrylbenzenes also serve as D and A units, respectively, which are capable of forming CTCs with bright fluorescence.[25] Alkoxy chains are bridged between them to block the π-conjugation and prevent possible structural defects in the luminophores. Homopolymers of both P(CHDCS) and P(CHDCSM) were directly produced on the electrode via the EP method and showed reversible FEC switching with remarkable contrast and fast response. The formation of CTCs between dicyanodistyrylbenzene and dimeric carbazole moieties with mixed-stacking pattern was found to play a key role in the FEC conversion. Electrochemical and spectroelectrochemical tests as well as theoretical calculations were further carried out to evaluate the effects of CTCs on the FEC performance.

2. Material and methods

2.1. Materials

Carbazole (96%), 1,6-dibromohexane (97%), 4-hydroxyphenylacetonitrile (98%), p-phthalaldehyde (98%), palladium acetate, tritertbutylphosphine, potassium iodide (99%), sodium methylate (97%) and lithium perchlorate ($LiClO_4$, 99%) were purchased from commercial sources and used as received. All solvents and other reagents (analytical grade) were used without further purification, unless otherwise claimed. Indium tin oxide (ITO) glass substrate (Kaivo Optoelectronic Technology Co., Ltd., Rs ≤ 15 Ω/sq) as working electrode was cleaned by ultrasonic in distilled water, ethanol, toluene and acetone solutions, successively.

2.2. Characterization

The ^1H and ^{13}C NMR spectra were recorded on a Bruker AVANCE III 500-MHz instrument (Bruker, Switzerland) using chloroform-d ($CDCl_3$) as the solvent and tetramethylsilane (TMS) as an internal standard. Mass spectroscopy was recorded on a Waters GCT Premier MS spectrometer using the electron impact (EI^+) technique. Fourier transform infrared spectrometer (FTIR) was recorded on a Nicolet 6700 (Thermo Fisher Nicolet, USA) with KBr pellets. The UV–vis absorption spectra were recorded on a Shimadzu UV-2600 spectrophotometer. Photoluminescent (PL) measurements were obtained on a SENS-9000 (Gilden Photonics, England). The time-resolved PL (TRPL) decay spectra were performed on an Edinburgh FLS980 fluorescence spectrometer. The electrochemical property measurement was recorded on an Ivium compactStat mobile measurement station (Ivium Technologies, Netherlands). The electrochemical measurements were performed in a conventional three-electrode cell contained 0.1 M $LiClO_4/CH_3CN$ or PC solution as the supporting electrolyte. The counter and reference electrodes in the three-electrode cell are Pt and Ag/AgCl electrodes respectively. UV–vis and PL spectroelectrochemical tests were carried out on the Ivium electrochemical analyzer integrated with a Shimadzu UV-2600 or a SENS-9000 PL spectrophotometer, respectively. The Gaussian 09 program was employed for DFT calculations. Geometry optimization was performed with the B3LYP functional, in combination with the D3BJ dispersion correction and Ahlrich's TZVP basis set. For the dicationic species, singlet and triplet states were both optimized and the open-shell singlet state was determined to be the ground state. The stability of wavefunction was examined for each compound. The spin density *iso*-surface was plotted at *iso*-value of 0.002.

2.3. Polymer synthesis and film deposition

Both P(CHDCS) and P(CHDCSM) polymeric thin films were prepared via electrochemical oxidative polymerization of respective monomers. The EP was performed in a conventional three-electrode cell with an ITO-coated glass as the working electrode which was successively washed with deionized water, ethanol, toluene and acetone under ultrasonication before use, a platinum (Pt) sheet and a double-junction Ag/AgCl electrode (silver wire coated with AgCl in saturated KCl solution) as the counter electrode and the reference electrode, respectively. A solution of 1.5 mM monomer in $CHCl_3/CH_3CN$ (1:4 vol%) with 0.1 M $LiClO_4$ as supporting electrolyte was prepared for electrochemical polymerization. Herein $CHCl_3$ was added to improve the solubility of CHDCS and CHDCSM monomers due to their poor solubility in acetonitrile solvent. The polymeric films were fabricated onto ITO-coated glass by cyclic voltammetry (CV) method within applied potential range of −0.5 to 1.35 V at a scan rate of 100 mV/s for 20 scan cycles. The resulting films were washed with $CHCl_3/CH_3CN$ (1:4 vol%) to remove unreacted precursors and supporting electrolytes.

2.4. FEC device fabrication

The prototype device with the area of (2 cm × 5 cm) possessing sandwich structure were assembled manually. The ITO-glass deposited with polymers serves as the working electrode, and the free ITO-glass is used as the counter electrode. A gel electrolyte was prepared with poly (methyl methacrylate) (PMMA, 3 g) and $LiClO_4$ (0.2 M) dissolving in

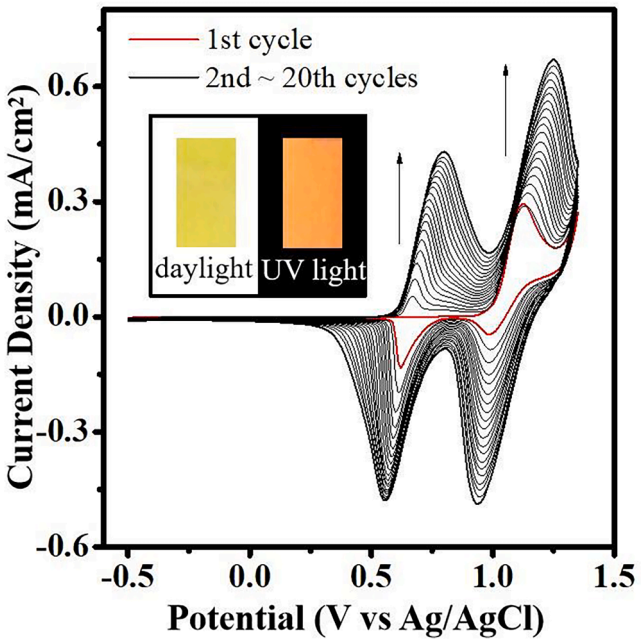

Fig. 1. CV profiles of CHDCS in $CHCl_3/CH_3CN$ (1:4 v/v) solution with $LiClO_4$ as the supporting electrolyte at a scanning rate of 100 mV/s.

propylene carbonate (PC, 5 g) to form a highly transparent and conductive gel. The gel electrolyte was spread on the polymer-coated side of the electrode, and sandwiched between the working electrode and counter electrode. An insulating frame of 3 M glue is placed between the two electrodes, which not only affords the space between them, but also makes the implementation of encapsulation.

3. Results and discussion

3.1. In-situ electro-polymerization

The monomers were synthesized by a sequence of C-N coupling, Williamson and Knoevenagel reactions, as shown in Scheme S1 in the Supporting information (SI). Detailed synthetic procedures and characterization results, including ^1H NMR, ^{13}C NMR, mass and infrared spectra, are provided in the experimental section. Bearing highly electroactive carbazole groups at both ends, both CHDCS and CHDCSM could be electropolymerized directly onto conducting substrates, forming uniform polymeric thin films. Fig. 1 shows the multicycle successive cyclic voltammetry (CV) curves of CHDCS in the range of −0.50 to 1.35 V with $LiClO_4$ as the supporting electrolyte. During the first cycle of the anodic scan, only one oxidative peak appears at 1.13 V, while starting from the second cycle, a new oxidative peak shows up at a lower potential of 0.67 V. The former peak originates from the formation of carbazole radical cations, which could couple with each other to form dimeric carbazole. The latter is attributed to the oxidation of the generated dimeric carbazole groups.[26] During the backward scans, two peaks appear at 0.99 and 0.62 V respectively, indicating that the biscarbazole dications are reduced to the neutral state via two one-electron steps.[27] After repeated CV cycles, a transparent light-yellowish film is observed on the electrode. The redox current is gradually increased in successive cycles, revealing the continuous coupling between the carbazole units and a gradual growth of the conductive polymer film. A slight increase in the peak potentials during the anodic process is attributed to the increase in resistance with the film thickening. Notably, two pairs of well-defined peaks remain even after 20 scanning cycles, suggesting that the electrochemical reactions only occur between

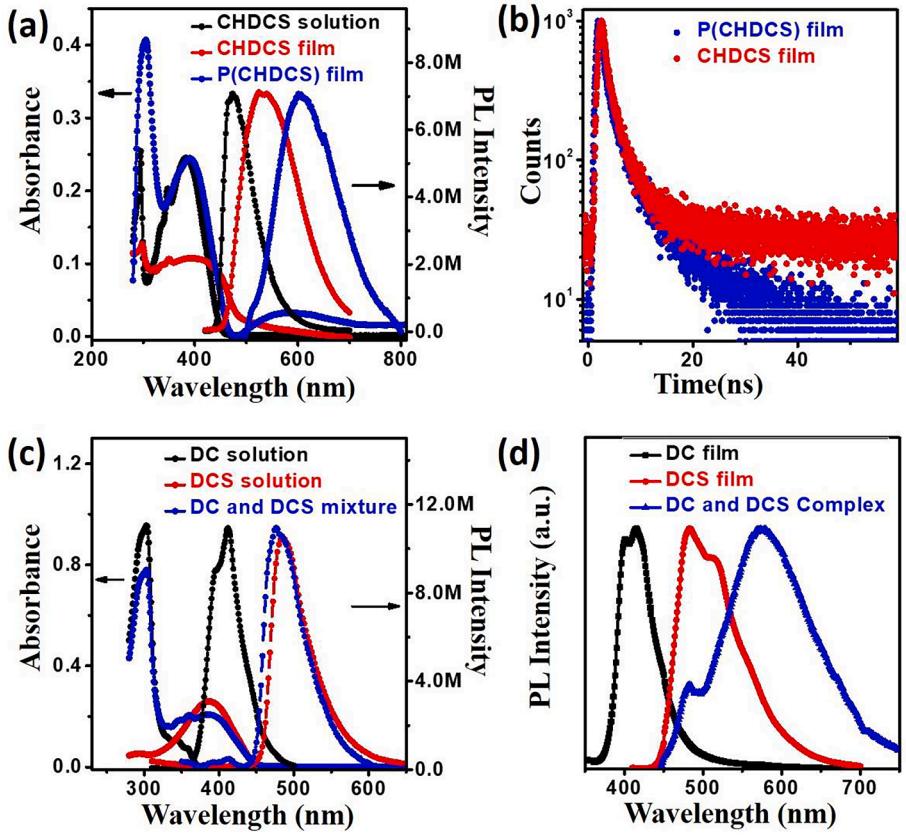

Fig. 2. (a) Absorption and PL spectra of CHDCS solution, CHDCS film and P(CHDCS) film. (b) TRPL of CHDCS and P(CHDCS) films. (c) Absorption and PL spectra of DC, DCS and their mixture in dilute solutions. (d) PL spectra of DC, DCS and their complexes in films.

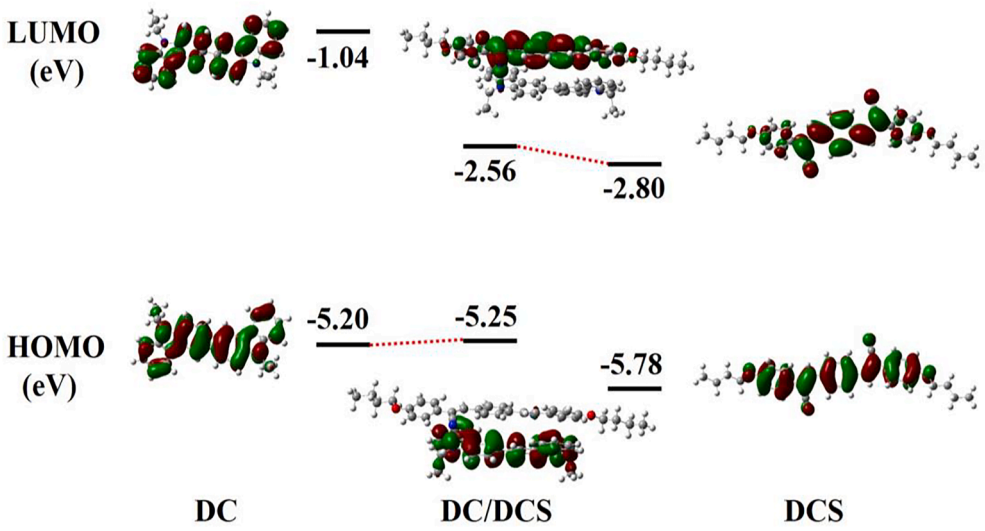

Fig. 3. The calculated energy levels and frontier molecular orbital diagrams of DC, DCS and their complexes.

carbazole units and also only dimeric carbazoles are formed instead of other oligomers. Therefore, the final products are the linear polymers P (CHDCS), as shown in Scheme 1. Likewise, P(CHDCSM) were also obtained via CV polymerization as shown in Figure S1 in the SI.

The polymer structures were further confirmed via FTIR spectra in comparison to their monomers. As shown in Figure S2, the peaks at 841 and 750 cm^{-1} in CHDCS monomer are attributed to para- and *ortho*-disubstituted benzene, respectively, which were also observed in P (CHDCS) yet with obvious red-shifts to 833 and 748 cm^{-1}, respectively. Additional peak appears at 800 cm^{-1} in P(CHDCS), indicating the generation of tri-substituted benzene, which is consistent with the coupled carbazole units.[28] Moreover, the intensity of tri-substituted benzene (800 cm^{-1}) is similar to that of *ortho*-disubstituted benzene (748 cm^{-1}), implying almost equal contents of these two moieties. These results confirm that the carbazole units form dimeric derivatives in the P (CHDCS) film. In addition, it is worth noting that the red-shifted peaks of P(CHDCS) relative to those of CHDCS indicate the negative charge of aromatic rings and the presence of CT interactions in the P(CHDCS) film, which agrees well with the following spectral analysis.

3.2. Charge-transfer complexes

Accordingly, EP was found to occur at carbazole units, resulting in polymers with isolated π-conjugations between bis-carbazoles and dicyanodistyrylbenzene moieties. In other words, the π-conjugation of polymers was not significantly extended with respect to that of their monomers. Surprisingly, the as-prepared EP film of P(CHDCS) instead displays a bright orange emission (λ_{max} = 603 nm) upon UV-light irradiation (Fig. 1), which is markedly red-shifted relative to that of CHDCS either in dilute solution (λ_{max} = 474 nm) or in thin film (λ_{max} = 524 nm), as shown in Fig. 2a. Moreover, the fluorescent lifetime is significantly shortened from 10.41 to 3.21 ns when CHDCS was polymerized into P (CHDCS), as determined by the time-resolved photoluminescence (TRPL) decays (Fig. 2b). The long-lived component (14.73 ns, 66.26%) in CHDCS, which is completely disappeared in P(CHDCS), results from the excimer emission of dicyanodistyrylbenzene units as described in the literature.[29] These results imply that the red-shifted emission of P (CHDCS) does not originate from the dicyanodistyrylbenzene core, no matter whether in dispersed or aggregated states. Rather, a mixed-stacking arrangement may be formed between dicyanodistyrylbenzene and bis-carbazole groups, which is supported by the characteristic absorption as shown in Fig. 2a. A new wide absorption band at approximately 580 nm is observed for the P(CHDCS) film, indicating the possibility of a CT transition.[30] Since the electron-rich (bis-carbazole) and electron-deficit (dicyanodistyrylbenzene) groups are separated by a non-conjugated alkoxy segment in P(CHDCS), the CT transition might result from CTCs formed between bis-carbazole and dicyanodistyrylbenzene units by stacking alternately on each other. To further verify whether the CT features originate from the CTCs, (2Z,2′Z)-3,3′-(1,4-phenylene)bis(2-(4-butoxyphenyl)acrylonitrile) (DCS) and 9,9′-diethyl-9H,9′H-3,3′-bicarbazole (DC) (Scheme 1) were synthesized and explored as components in P(CHDCS).

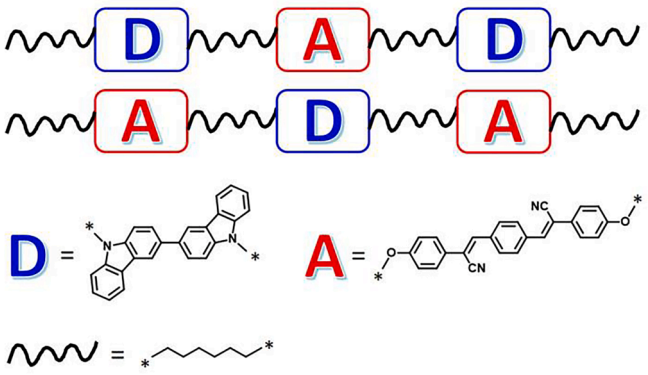

Scheme. 2. Schematic illustration of the possible structure of the interchain CTCs with mixed D-A stacks in P(CHDCS) thin film.

A mixture of DC and DCS in solution display both the absorption and PL spectra, which is essentially the sum of the respective spectra of DC and DCS (Fig. 2c). The emission of DC in the mixed solution is greatly decreased in intensity via energy transfer due to a large overlap of its PL with the absorption of DCS. However, when the mixed solution was drop-casted on a glass substrate, orange fluorescence with a significantly red-shifted and broad PL was observed after solvent evaporation (Fig. 2d). The newly generated PL peak at λ_{max} = 577 nm is completely different from those of either DC or DCS, verifying the formation of CTCs between them in solid states.[31] Given the optical property of CTCs is determined by the relative molecular orbital offset of D and A pairs, DFT calculations were further performed.[32,33] The energy level diagrams for DC and DCS as well as their complexes are schematically shown in Fig. 3. From the oxidation potential of bis-carbazole at 0.67 V in CV, we can estimate the highest occupied molecular orbital (HOMO) level as −5.11 eV by assuming the Ag/AgCl reference to be −4.44 eV.[34] This agrees well with the calculation shown in Fig. 3. The HOMO energy level

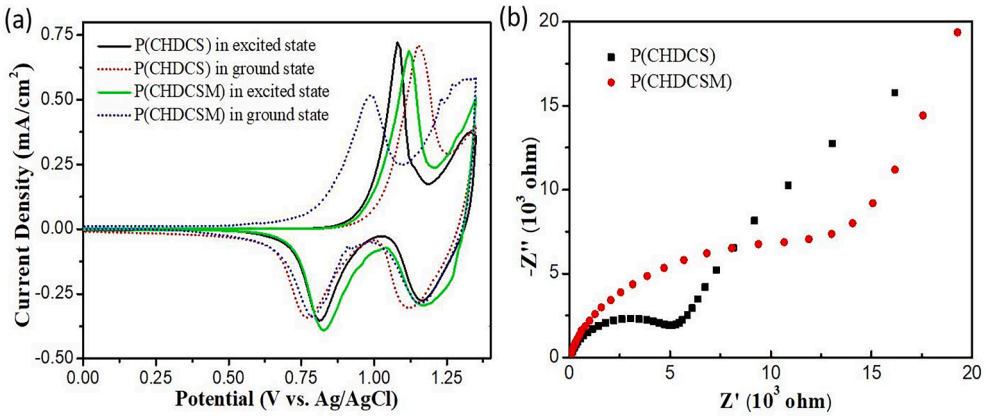

Fig. 4. (a) CVs of polymer films in different states in 0.1 M $LiClO_4/CH_3CN$ solution at a scan rate of 25 mV/s. (b) EIS spectra of P(CHDCS) and P(CHDCSM).

of the mixed-stacking DC/DCS complex is estimated to be −5.25 eV, which is closer to that of the DC donor (-5.20 eV), while the lowest-unoccupied molecular orbital (LUMO) (-2.56 eV) is much more similar to that of the DCS acceptor (-2.80 eV). Moreover, the HOMO level of the complex is primarily located on the DC donor, while the LUMO is distributed on the DCS acceptor, indicating the CT transition from DC to DCS. These results reveal that the bis-carbazole and dicyanodistyrylbenzene units in P(CHDCS), analogous to the DC and DCS pair, are prone to form CTCs and emit remarkably red-shifted CT fluorescence. This finding is consistent with the optical properties of the P(CHDCS) film, as mentioned above.

Accordingly, a possible aggregated structure of the polymers is shown in Scheme 2, in which the bis-carbazole and dicyanodistyrylbenzene segments are proposed to be sandwiched between one another to form interchain CTCs. The ionic electrostatic repulsion between oxidized bis-carbazoles, which is generated during the EP process, promotes the formation of such CTCs, along with the driving forces of CT and π-π interactions between bis-carbazole and dicyanodistyrylbenzene units. As a result, a strong luminescence is observed from P(CHDCS) due to the CT transition occurring by an electron transfer from the HOMO level of bis-carbazole to the LUMO level of dicyanodistyrylbenzene. Compared to P(CHDCS), P(CHDCSM) shows a weak CT transition in the absorption spectrum (Figure S3), indicative of its weak CT character in the ground state. However, in the excited-state, P(CHDCSM) still displays similar bright orange fluorescence (at ca. 600 nm) and decreased fluorescent lifetime (from 9.96 ns in monomer to 5.0 ns in polymer). This suggests that alternate D/A stacks may also be formed in P(CHDCSM), which exhibits the excited-state CT character. The introduction of bulky $–OCH_3$ groups in P(CHDCSM) not only suppress the close stacking between D and A segments, but also weakens the electron-withdrawing capacity of the A part. Consequently, P(CHDCSM) has a relatively weak CT which requires light excitation. Since the CT interaction is significantly affected by the charged states of the CTCs, the fluorescence from the CT transition is assumed to be regulated by electrochemical reactions. This hypothesis will be verified in the following experiments.

3.3. Electrochemical analysis

The CVs of the EP polymers was investigated and the results are shown in Figure S5 and 4a. No obvious oxidation and reduction at the negative potential from −1.35 to 0 V is observed for both P(CHDCS) and P(CHDCSM) films. However, at the positive potential, all CV curves display a sequence of two quasi-reversible redox events. The first oxidation wave presumably corresponds to the formation of bis-carbazole radical cations while the second refers to further oxidation to bis-carbazole dications (Figure S6). We also compared the CVs of polymers with and without UV light excitation and the corresponding peak potentials are summarized in Table S1. Note that the oxidation potential of P(CHDCSM) in the ground state is lower than that in its excited state as well as those of P(CHDCS), all of which have significant CT features. This indicates that P(CHDCSM) performs better electrochemical activity under lower applied potentials due to the almost absent CT in the ground state. Moreover, the UV light-excited P(CHDCS) shows a decreased oxidation potential of E_{pa} = 1.08 V and an increased reduction potential of E_{pc} = 0.81 V, resulting in a smaller potential separation of 0.27 V between the oxidation and reduction peaks in comparison to those without light excitation (0.38 V). These results suggest that the CT interaction between bis-carbazole and dicyanodistyrylbenzene units impedes the oxidation reactions, which however occur with better activity and reversibility upon UV-illumination due to the intermolecular CT transition at the D/A interface.[35] In addition, the scanning rate-dependent CVs in the range of 25–200 mV/s for P(CHDCS) and 25–400 mV/s for P(CHDCSM) films were obtained as shown in Figure S7 and 8. A linear relationship is found between the square roots of the scanning rate and the peak currents, demonstrating that the electrochemical processes are diffusion limited in such a range of scanning rates. The diffusion limitation might be attributed to the slow diffusion of the counter-ions ClO_4^- from electrolyte solution into the polymeric films to preserve electroneutrality.

The electrochemical impedance spectra (EIS) of polymers in the frequency range from 0.1 to 1000 kHz are shown in Fig. 4b. Both polymers exhibited EIS spectra consisting of a semicircle at high frequencies and an inclined line at low frequencies, which corresponds to the CT resistance across the film (R_{ct}) and the diffusion resistance of the electrolyte ions into the electrode (Warburg impedance Z_w), respectively.[7] This indicates that the electrochemical reactions of the polymers are under kinetic control at high frequencies and mass transfer control at low frequencies. The equivalent circuit of EIS have been provided in Figure S9 together with the summary of EIS fitting results in Table S2 in SI. It is obvious that P(CHDCS) shows a much smaller R_{ct} than P(CHDCSM) owing to its stronger CT. Therefore, an incorporation of bulky $–OCH_3$ groups on the conjugated plane can hinder the close π-stacking and charge transfer between D and A segments, which leads to a higher R_{ct} resistance of P(CHDCSM) films. The better electrical conductivity of P(CHDCS) is believed to facilitate its FEC response, as discussed below.

3.4. FEC switching

Figure S10 shows the patterned polymer film of 'ZJHU' (i.e., Huzhou University at ZheJiang), which was simply prepared from the CHDCS monomer via one-step in-situ EP. Interestingly, high-performance FEC behaviors are observed, in which the on/off fluorescence switching occurs contemporaneously with color conversion between yellow and green at 0 V and 1.35 V, respectively. This indicates that the redox of the

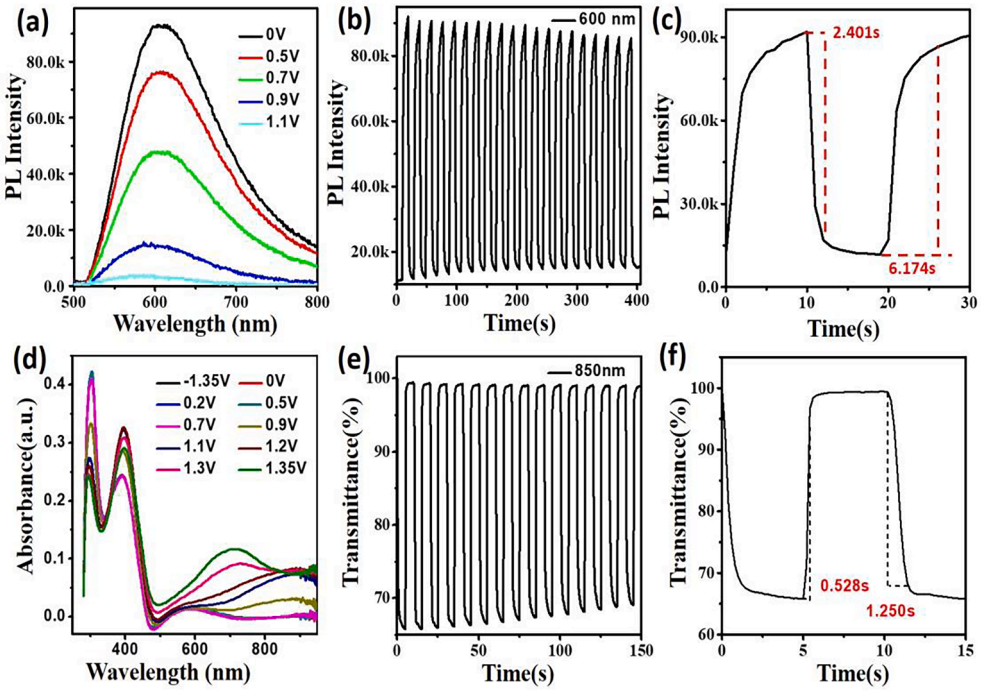

Fig. 5. (a) PL spectra of the P(CHDCS) film under different potentials. (b) PL intensity contrast and (c) switching time of the P(CHDCS) film in 0.1 M $LiClO_4/CH_3CN$ solution under stepping potentials between −0.5 V and 1.35 V with intervals of 10 s. (d) Absorption spectra of P(CHDCS) film under different potentials. (e) Transmittance contrast and (f) switching time of P(CHDCS) film under stepping potentials between −0.5 V and 1.35 V with intervals of 5 s.

bis-carbazole moiety in P(CHDCS) induces both color and CT fluorescence changes. These optical changes are large enough to be easily distinguished by the naked eye.

Fig. 5 and Figure S11,12 show the voltage-dependent PL and absorption spectra of the P(CHDCS) and P(CHDCSM) films, respectively. For P(CHDCS), bright orange fluorescence (λ_{max} = 603 nm) is found in the neutral state at 0 V (Fig. 5a). As the applied potential is increased to 0.5 V, the PL intensity is dropped, which is further greatly weakened and even approaches the baseline as the potential reaches 1.1 V, resulting in a nearly quenched dark state. The contrast of the PL intensity (I_{on}/I_{off}) at 603 nm is as large as 28.3. Note that such fluorescent changes could be recovered. Repetitive PL switching of the P(CHDCS) film was tested upon cyclic potential step between −0.5 V and 1.35 V. As shown in Fig. 5b, large intensity variation and good reversibility with little decay even after 20 cycles are displayed during the potential step, revealing the advantageous fatigue resistance of fluorescent switching. Fig. 5c shows the response curves of P(CHDCS) film, in which the response time is estimated to be 95% of the full change in PL intensity. The P(CHDCS) film shows a rapid quenching speed (2.401 s) and a slow brightening speed (6.174 s). Similar fluorescent changes are also observed in the P(CHDCSM) film (Figure S9), which nevertheless show a much smaller contrast and worse reversibility after several cycles. The I_{on}/I_{off} decays from 12.5 in the first cycle to 4.8 after 20 cycles. In one cycle, only 70% of PL intensity could be recovered upon −0.5 V for 5 s, which is considered as the main cause of the large decay of P(CHDCSM) after several cycles. The poor reversibility might be attributed to the high R_{ct} resistance of P(CHDCSM) film.

As the fluorescence is changed, the absorption is also varied depending on the applied potential, as illustrated in Fig. 5d-f and Figure S10. Taking P(CHDCS) as an example, a maximum absorption peak at 395 nm appears concomitantly with a weak shoulder band at 580 nm in the neutral state at 0 V, resulting in a yellowish color under natural light. The peak at shorter wavelengths is attributed to the π-π* transition of the dicyanodistyrylbenzene moiety, in consistence with Fig. 2c. The shoulder band at longer wavelengths is due to the CT transition from bis-carbazoles to dicyanodistyrylbenzene groups in adjacent molecules, as mentioned above. When the applied potential is increased above 0.7 V, a new absorption band appears at 850 nm, which is further enhanced in intensity to reach a maximum at a potential of 1.2 V. When the voltage rises continuously up to 1.3 V, another broad band appears at about 700 nm and is then gradually intensified. The generation of these two new absorption bands at 850 and 700 nm is ascribed to the formation of polaron and bipolaron, respectively (Figure S6).[36] Finally, a green color of P(CHDCS) shows up and becomes stronger with an increasing potential. Fig. 5e shows the repetitive transmittance switching of the P(CHDCS) film upon cyclic potential steps between −0.5 V and 1.35 V. The contrast of transmittance (ΔT) at 850 nm is shown to exceed 33%. Superior to the fluorescent switching, the P(CHDCS) film exhibited a much faster EC response with a coloring time of 1.250 s and a fading time of 0.528 s. As for P(CHDCSM) film, similar color switching between yellow and green with an optical contrast of 31% and response times of 1.253 and 0.512 s are observed in Figure S12. Both of P(CHDCS) and P(CHDCSM) show almost the identical EC switching behaviors, which originate from the same EC-active groups-biscarbazole.

However, as for the EC stability, P(CHDCS) and P(CHDCSM) display distinct performance. Figure S13 shows the changes of optical contrast in both P(CHDCS) and P(CHDCSM) under 200 cycles of potentiostatic step. P(CHDCS) retains 95.6% of its original optical contrast after 100 cycles, and abruptly decays after 120 cycles. 46.3% of its original optical contrast is left even after 150 cycles. However, P(CHDCSM) appears to decay rapidly, remaining only 62.9 % and 3.2% of its original optical contrast after 100 and 150 cycles respectively. The fast attenuation of P(CHDCSM) is attributed to the partially polymer dissolution caused by the repeated doping/de-doping process, which is proved by the thinner films after tests. These results indicate better stability of P(CHDCS) in comparison to P(CHDCSM), which might result from the stronger interchain CT interactions in P(CHDCS) that prevent the dissolution of polymers.

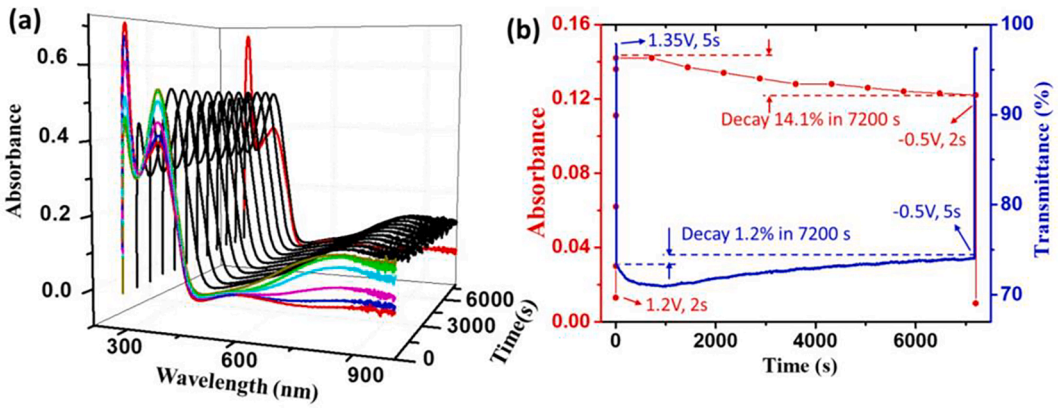

Fig. 6. (a) Absorption spectra of P(CHDCS) upon electrical triggering with + 1.2 V for 2 s, power off for 2 h and −0.5 V for 2 s. (b) The absorbance and transmittance of P(CHDCS) at 850 nm under different electrical triggering.

3.5. Color stability

An unusual color stability is observed for the P(CHDCS) film, which maintains the colored state for a particularly long period without a power supply. As shown in Fig. 6a, the absorption spectra were measured by triggering with 1.2 V for 2 s, followed by power off for 2 h until the negative voltage (-0.5 V for 2 s) was applied. The intensity of the absorption band at 850 nm is gradually increased during the current triggering step and exhibits a small decay of 14.1% when the power was cut off for 2 h (Fig. 6b). Then, the spectra were recovered quickly upon stimulation with −0.5 V for 2 s. The stability could be further improved by adjusting the applied voltage and time. After electrical triggering by 1.35 V for 5 s, the power was cut off, and the transmittance at 850 nm exhibits a decay of only 1.2% in 2 h before a negative voltage of −0.5 V was applied for 5 s. Note that the transmittance is spontaneously decreased a bit for a few minutes after the current supply was stopped, which leads to a further decrease of color attenuation. These results indicate the long-lasting information display and optical memory of the FEC P(CHDCS) film with only a small energy consumption, which is favorable for energy-efficient devices.

The persistent display is related to the stability of bis-carbazole cationic radicals in this electrochemical system. However, such stable π-conjugations with open-shell electronic structures have barely been reported. To gain an in-depth understanding of the mechanism, theoretical analysis of the electronic configuration of cationic radicals was further conducted. It is found that the spin density of the mono-radical cation (polaron) is mainly delocalized on two N-atoms and their intervening phenyl rings with very small amounts on the other peripheral benzenes (Figure S14). This implies that the second carbazole fragment aids to stabilize the radical by a resonance effect, causing the 6-position in the carbazoles to be inactive. Moreover, the unpaired electron is even slightly delocalized across the adjacent dicyanodistyrylbenzene units in the CTC system, which further stabilizes the radical via CT. In addition, the mixed-stacking arrangement in CTCs effectively prevents the radicals from reacting with each other. These results are also supported by the above-mentioned CV profiles, which show a reversible oxidation process forming bis-carbazole cationic radicals. With regards to the improved color stability at 1.35 V, the prolonged decrease in transmittance is assigned to the conversion from the bipolaron pattern (λ_{abs} = 700 nm) to a diradical cation that could be treated as two monopolarons (λ_{abs} = 850 nm) owing to the presence of two carbazole radical cations.[37] The two-electron oxidized bis-carbazole indeed shows a spin density difference, with each unpaired electron residing mainly on one carbazole unit and only slightly delocalizing over the second one, suggestive of the biradicaloid nature (Figure S14b).

4. Conclusions

To conclude, we have designed and demonstrated a new class of FEC polymers based on CTCs bearing mixed D-A stacks that are readily fabricated through electrochemical polymerization. The EP films exhibit a bright orange fluorescence arising from the intermolecular CT excitons formed between dicyanodistyrylbenzene and bis-carbazole segments, which could be electrically modulated. Moreover, stronger intermolecular CT effectively improves the electrical conductivity and thus accelerates the FEC response of polymers, leading to a large fluorescent contrast of 28.3 and high reversibility. Meanwhile, the color is transformed between light yellow and green with rapid response times of 1.25 s for coloring and 0.53 s for fading. In addition, the FEC thin films exhibit good color stability with the colored state decaying by only 1.2% in 2 h without a power supply thanks to the improved spin delocalization and the blocked radical pairing by CTC mixed-stacks, which is favorable for energy-efficient devices.

Declaration of Competing Interest

The authors declare that they have no known competing financial interests or personal relationships that could have appeared to influence the work reported in this paper.

Acknowledgments

We acknowledged the support of Science and Technology Commission of Shanghai Municipality (STCSM) under grant No. 20XD1400500 (Z.L.), National Natural Science Foundation of China (NSFC)-The Swedish Foundation for International Cooperation in Research and Higher Education (STINT) under grant No. 5191101797 (Z.L.) and National Natural Science Foundation of China (51803056) (J.S.).

Appendix A. Supplementary data

Supplementary data to this article can be found online at https://doi.org/10.1016/j.cej.2021.132625.

References

[1] A. Beneduci, S. Cospito, M. La Deda, L. Veltri, G. Chidichimo, Electrofluorochromism in π-conjugated ionic liquid crystals, Nat. Commun. 5 (2014) 3105.
[2] J. Zhang, Z. Chen, X.-Y. Wang, S.-Z. Guo, Y.-B. Dong, G.-A. Yu, J. Yin, S.-H. Liu, Redox-modulated near-infrared electrochromism, electroluminochromism, and aggregation-induced fluorescence change in an indolo[3,2-b]carbazole-bridged diamine system, Sensor. Actuat. B-Chem. 246 (2017) 570–577.
[3] J. Sun, Y. Chen, Z. Liang, Electroluminochromic materials and devices, Adv. Funct. Mater. 26 (2016) 2783–2799.

[4] T. Yu, Y. Han, H. Yao, Z. Chen, S. Guan, Polymeric optoelectronic materials with low-voltage colorless-to-black electrochromic and AIE-activity electrofluorochromic dual-switching properties, Dyes Pigments 181 (2020), 108499.
[5] N. Sun, K. Su, Z. Zhou, Y.e. Yu, X. Tian, D. Wang, X. Zhao, H. Zhou, C. Chen, AIE-active polyamide containing diphenylamine-TPE moiety with superior electrofluorochromic performance, ACS Appl. Mater. Interfaces 10 (2018) 16105–16112.
[6] H.-J. Yen, C.-J. Chen, G.-S. Liou, Novel high-efficiency PL polyimide nanofiber containing aggregation-induced emission (AIE)-active cyanotriphenylamine luminogen, Chem. Commun. 49 (2013) 630–632.
[7] J. Sun, Z. Liang, Swift electrofluorochromism of donor–acceptor conjugated polytriphenylamines, ACS Appl. Mater. Interfaces 8 (2016) 18301–18308.
[8] S. Mi, J. Wu, J. Liu, Z. Xu, X. Wu, G. Luo, J. Zheng, C. Xu, AIEE-active and electrochromic bifunctional polymer and a device composed thereof synchronously achieve electrochemical fluorescence switching and electrochromic switching, ACS Appl. Mater. Interfaces 7 (2015) 27511–27517.
[9] X.u. Yang, S. Seo, C. Park, E. Kim, Electrical chiral assembly switching of soluble conjugated polymers from propylenedioxythiophene-phenylene copolymers, Macromolecules 47 (2014) 7043–7051.
[10] Y. Liu, Y. Wei, M. Liu, Y. Bai, X. Wang, S. Shang, J. Chen, Y. Liu, Electrochemical synthesis of large area two-dimensional metal–organic framework films on copper anodes, Angew. Chem. Int. Ed. 60 (2021) 2887–2891.
[11] S. Yan, H. Fu, L. Zhang, Y. Dong, W. Li, M. Ouyang, C. Zhang, Conjugated polymer multilayer by in situ electrochemical polymerization for black-to- transmissive eletrochromism, Chem. Eng. J. 406 (2021), 126819.
[12] N. Xu, S. Mei, Z. Chen, Y. Dong, W. Li, C. Zhang, High-performance Li-organic battery based on thiophene-containing porous organic polymers with different morphology and surface area as the anode materials, Chem. Eng. J. 395 (2020), 124975.
[13] C. Gu, W. Dong, L. Yao, Y. Lv, Z. Zhang, D. Lu, Y. Ma, Cross-linked multifunctional conjugated polymers prepared by in situ electrochemical deposition for a highly-efficient blue-emitting and electron-transport layer, Adv. Mater. 24 (2012) 2413–2417.
[14] Q. Lu, C. Yang, X. Qiao, X.u. Zhang, W. Cai, Y.e. Chen, Y. Wang, W. Zhang, X. Lin, H. Niu, W. Wang, Multifunctional AIE-active polymers containing TPA-TPE moiety for electrochromic, electrofluorochromic and photodetector, Dyes Pigments 166 (2019) 340–349.
[15] C. Xia, R.C. Advincula, A. Baba, W. Knoll, Electrochemical patterning of a polyfluorene precursor polymer from a microcontact printed (μCP) monolayer, Chem. Mater. 16 (2004) 2852–2856.
[16] J.-J. Huang, H.-A. Lin, C. Chen, P.-W. Tang, S.-C. Luo, Corannulene-based donor–acceptor-type conjugated polymers with electrochromic properties, J. Mater. Chem. C 9 (2021) 7919–7927.
[17] W. Wang, L. Luo, P. Sheng, J. Zhang, Q. Zhang, Multifunctional features of organic charge-transfer complexes: advances and perspectives, Chem. Eur. J. 27 (2021) 464–490.
[18] Y.-L. Lei, Y. Jin, D.-Y. Zhou, W. Gu, X.-B. Shi, L.-S. Liao, S.-T. Lee, White-light emitting microtubes of mixed organic charge-transfer complexes, Adv. Mater. 24 (2012) 5345–5351.
[19] S. Horiuchi, Y. Okimoto, R. Kumai, Y. Tokura, Quantum phase transition in organic charge-transfer complexes, Science 299 (2003) 229–232.
[20] J. Han, D. Yang, X. Jin, Y. Jiang, M. Liu, P. Duan, Enhanced circularly polarized luminescence in emissive charge-transfer complexes, Angew. Chem. Int. Ed. 58 (2019) 7013–7019.
[21] J. Wang, S. Zhang, S. Xu, A. Li, B. Li, L. Ye, Y. Geng, Y. Tian, W. Xu, Morphology-dependent luminescence and optical waveguide property in large-size organic charge transfer cocrystals with anisotropic spatial distribution of transition dipole moment, Adv. Optical Mater. 17 (2020) 1901280.
[22] W. Chen, B. Huang, S. Ni, Y. Xiong, A.L. Rogach, Y. Wan, D. Shen, Y. Yuan, J. Chen, M. Lo, C. Cao, Z. Zhu, Y. Wang, P. Wang, L. Liao, C. Lee, Deep-red/near-infrared electroluminescence from single-component charge-transfer complex via thermally activated delayed fluorescence channel, Adv. Funct. Mater. 29 (2019) 1903112.
[23] D. Yan, A. Delori, G.O. Lloyd, T. Friščić, G.M. Day, W. Jones, J. Lu, M. Wei, D. G. Evans, X. Duan, A cocrystal strategy to tune the luminescent properties of stilbene type organic solid-state materials, Angew. Chem. Int. Ed. 50 (2011) 12483–12486.
[24] I.M. Khan, S. Shakya, R. Akhtar, K. Alam, M. Islam, N. Alam, Exploring interaction dynamics of designed organic cocrystal charge transfer complex of 2-hydroxypyridine and oxalic acid with human serum albumin: single crystal, spectrophotometric, theoretical and antimicrobial studies, Bioorg. Chem. 100 (2020), 103872.
[25] M.S. Kwon, J. Gierschner, S. Yoon, S.Y. Park, Unique piezochromic fluorescence behavior of dicyanodistyrylbenzene based donor-acceptor-donor triad: mechanically controlled photo-induced electron transfer (eT) in molecular assemblies, Adv. Mater. 24 (2012) 5487–5492.
[26] H. Zhang, Y. Zhang, C. Gu, Y. Ma, Electropolymerized conjugated microporous poly(zinc-porphyrin) films as potential electrode materials in supercapacitors, Adv. Energy Mater. 5 (2015) 1402175.
[27] C. Gu, N. Huang, Y. Wu, H. Xu, D. Jiang, Design of highly photofunctional porous polymer films with controlled thicknessand prominent microporosity, Angew. Chem. Int. Ed. 54 (2015) 11540–11544.
[28] C. Gu, Y. Chen, Z. Zhang, S. Xue, S. Sun, K. Zhang, C. Zhong, H. Zhang, Y. Pan, Y. Lv, Y. Yang, F. Li, S. Zhang, F. Huang, Y. Ma, Electrochemical route to fabricate film-like conjugated microporous polymers and application for organic electronics, Adv. Mater. 25 (2013) 3443–3448.
[29] M. Kinami, B.R. Crenshaw, C. Weder, Polyesters with built-in threshold temperature and deformation sensors, Chem. Mater. 18 (2006) 946–955.
[30] D. Li, W. Hu, J. Wang, Q. Zhang, X.-M. Cao, X. Ma, H.e. Tian, White-light emission from a single organic compound with unique self-folded conformation and multistimuli responsiveness, Chem. Sci. 9 (2018) 5709–5715.
[31] X. Han, F. Hu, W. Chi, X. Ma, S.H. Liu, X. Liu, J. Yin, Unusual intermolecular charge transfer enables supramolecular fluorescent viscosity sensors, Sensor. Actuat. B-Chem. 277 (2018) 55–61.
[32] S.K. Park, J.H. Kim, T. Ohto, R. Yamada, A.O.F. Jones, D.R. Whang, I. Cho, S. Oh, S. H. Hong, J.E. Kwon, J.H. Kim, Y. Olivier, R. Fischer, R. Resel, J. Gierschner, H. Tada, S.Y. Park, Highly luminescent 2D-type slab crystals based on a molecular charge-transfer complex as promising organic light-emitting transistor materials, Adv. Mater. 29 (2017) 1701346.
[33] L. He, R. Bai, R. Yu, X. Meng, M. Tian, X. Wang, Donor/acceptor pairs created by electrostatic interaction: design, synthesis, and investigation on the exciplex formed within the pair, Angew. Chem. Int. Ed. 60 (2021) 6013–6020.
[34] H. Meng, J. Zheng, A.J. Lovinger, B.-C. Wang, P.G. Van Patten, Z. Bao, Oligofluorene-Thiophene Derivatives as High-Performance Semiconductors for Organic Thin Film Transistors, Chem. Mater. 15 (2003) 1778–1787.
[35] H.I. Karunadasa, C.J. Chang, J.R. Long, A molecular molybdenum-oxo catalyst for generating hydrogen from water, Nature 464 (2010) 1329–1333.
[36] J. Sun, X. Lv, P. Wang, Y. Zhang, Y. Dai, Q. Wu, M. Ouyang, C. Zhang, A donor-acceptor cruciform π-system: high contrast mechanochromic properties and multicolour electrochromic behavior, J. Mater. Chem. C 2 (2014) 5365–5371.
[37] S. Kasemthaveechok, L. Abella, M. Jean, M. Cordier, T. Roisnel, N. Vanthuyne, T. Guizouarn, O. Cador, J. Autschbach, J. Crassous, L. Favereau, Axially and helically chiral cationic radical bicarbazoles: SOMO-HOMO level inversion and chirality impact on the stability of mono- and diradical cations, J. Am. Chem. Soc. 142 (2020) 20409–20418.